Emission enhancement in Er³⁺/Pr³⁺-codoped germanate glasses and their use as a 2.7-μm laser material

Xiangtan Li (李响潭)[1,2], **Xueqiang Liu (刘雪强)**[1,2], **Liyan Zhang (张丽艳)**[1], **Lili Hu (胡丽丽)**[1], **and Junjie Zhang (张军杰)**[1*]

[1]*Key Laboratory of Materials for High Power Laser, Shanghai Institute of Optics and Fine Mechanics,*
Chinese Academy of Sciences, Shanghai 201800, China

[2]*Graduate University of Chinese Academy of Science, Beijing 100049, China*

*Corresponding author: jjzhang@mail.siom.ac.cn

Received August 29, 2013; accepted October 17, 2013; posted online November 20 , 2013

Emission enhancement at 2.7 μm is observed in Er³⁺/Pr³⁺-codoped germanate glasses when pumped by a 980-nm laser diode. Significant reductions in 1.5-μm emission and upconversion intensity indicate efficient energy transfer between Er³⁺ and Pr³⁺; the energy transfer efficiency is as high as 77.4%. The mechanisms of energy transfer are discussed in detail. The calculated emission cross-section of Er³⁺/Pr³⁺-codoped germanate glass is 8.44×10^{-21} cm², which suggests that Er³⁺/Pr³⁺-codoped germanate glass can be used to achieve efficient 2.7-μm emission.

OCIS codes: 160.2290, 160.5690, 300.2140.

doi: 10.3788/COL201311.121601.

Increasing interest has been given to 2.7-μm fibers because of their wide range of applications in surgery, the military, fiber communications, and monitoring of atmospheric contaminants[1]. New types of laser glass serving as mid-infrared (IR) hosts have also been developed. ZBLAN glass is a candidate material that may potentially be applied in Er³⁺-doped 2.7-μm fiber lasers[2−4]. Fluorophosphate, chalcogenide, and tellurite glasses also exhibit 2.7-μm fluorescence[5−7]. Despite this property, however, ZBLAN and chalcogenide glasses have unsatisfactory thermal and chemical stabilities, and tellurite glass is fragile.

Similar to tellurite glass, germanate glass has a low phonon energy as well as good thermal stability and chemical durability. These desirable qualities indicate that germanate glass may be applied in mid-IR lasers. Unfortunately, –OH groups in oxide glass hosts often eliminate 2.7-μm emission. Thus, fluoride is commonly added to germanate glass matrices to reduce their OH⁻ contents.

Corresponding to a ⁴I₁₁/₂ →⁴I₁₃/₂ transition, Er³⁺ 2.7-μm emission, which is considered "self-terminating," cannot be obtained efficiently. Doping with rare-earth ions, such as Ho³⁺, Yb³⁺, Tm³⁺, and Nd³⁺, which have energy levels approximately equal to that of ⁴I₁₃/₂, have been demonstrated to solve this problem[5,8−10]. Thus, codoping with Pr³⁺ may be expected to enhance 2.7-μm emissions.

In this letter, Er³⁺/Pr³⁺ (EP)-codoped germanate glasses with molar compositions of 56GeO₂–15PbO–14Na₂O–12Ga₂O₃–3PbF₂–Er₂O₃–xPr₂O₃ (x=0,0.1,0.2, 0.5, labeled EP0, EP1, EP2, and EP5, respectively) were melted. The syntheses and measurement methods of the EP glasses are identical to those described in Ref. [9].

The absorption spectra of Er³⁺-doped and EP-codoped germanate glasses are shown in Fig. 1; in the figure, absorption bands attributed to the transitions of Er³⁺ and Pr³⁺ ions from the ground state are labeled. Er³⁺ shows

similar absorption bands in the samples, and Pr³⁺ absorption peaks at approximately 600 and 1500 nm are found in the spectra of the codoped samples. The specific absorption bands are also enhanced by increases in Pr³⁺ content. Absorption bands at approximately 980 nm indicate that the glass samples may be efficiently excited by a 980-nm laser diode.

The radiative transition of the 4fⁿ–4fⁿ configuration of a rare-earth ion has been analyzed in accordance with Judd–Ofelt theory[11]. The least-squares method may be generally applied to fit the measured oscillator strengths of absorption bands. The transition ground state ⁴I₁₅/₂ to ⁴I₁₃/₂ is excluded. The root-mean-square error is equal to 0.1×10^{-6}, which indicates that the results are reliable. The Judd–Ofelt parameters Ω_λ are obtained from the measured absorption spectra in this letter. The obtained parameters are $\Omega_2 = 6.60 \times 10^{-20}$ cm², $\Omega_4 = 1.75 \times 10^{-20}$ cm², and $\Omega_6 = 0.99 \times 10^{-20}$ cm². Using Judd–Ofelt intensity parameters, the radiative transition probability (A_{rad})

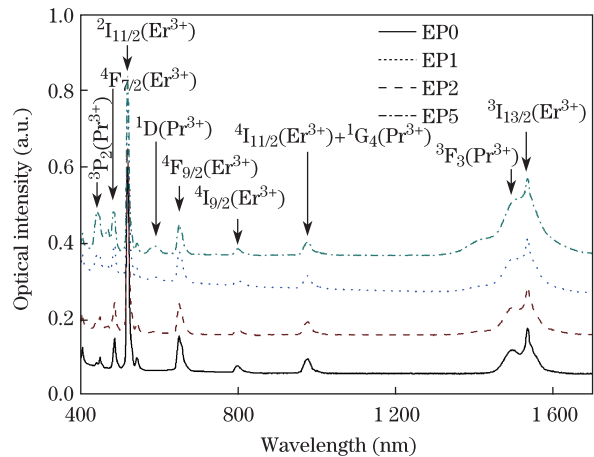Fig. 1. Absorption spectra of Er³⁺ and EP-codoped samples.
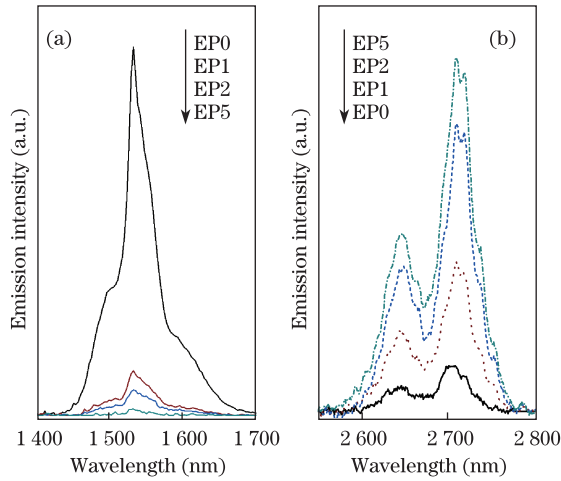
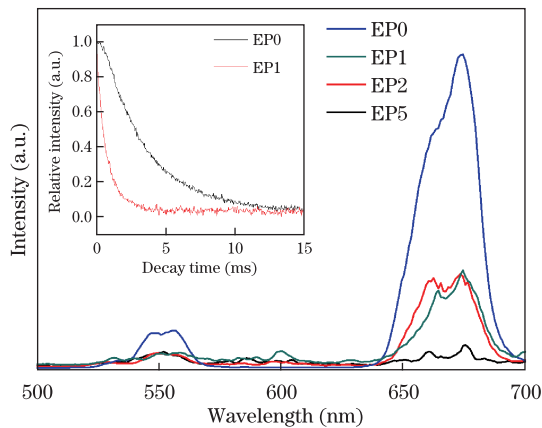Fig. 2. IR PL spectra in the (a) 1.5- and (b) 2.7-μm region of Er^{3+}- and EP-doped glasses.

Fig. 3. Upconversion spectra of EP-doped glass. Inset: decay time in Er^{3+}-doped and EP-codoped glasses.

and branching ratios (β) of the Er^{3+}:$^4I_{11/2} \rightarrow ^4I_{13/2}$ transition for the codoped sample are calculated as 36.69 s^{-1} and 16.71%, respectively.

The IR photoluminescence (PL) spectra of Er^{3+}-doped and EP-codoped glasses are shown in Fig. 2. Emission peaks centered at 1550 and 2710 nm may be observed. In the Er^{3+}-doped glass (EP0), very slight 2.7-μm emission from the excited energy level $^4I_{11/2}$ may be observed, and intense PL from $^4I_{13/2}$ is measured. This phenomenon indicates the highly efficient nonradiative relaxation of $^4I_{11/2}$ to $^4I_{13/2}$. In Fig. 2(a), a significant reduction in emission intensity of $^4I_{13/2}$ level may be observed. The intensity of 1550-nm emission decreases with increasing Pr^{3+} concentration. Figure 2(b) shows significant enhancements in 2.7-μm emission with increasing addition of Pr^{3+}. This observation suggests that Pr^{3+} ions can be used effectively to depopulate the Er^{3+}:$^4I_{13/2}$ level.

The PL decay curves of the Er^{3+}:$^4I_{13/2}$ levels of the Er^{3+}-doped and EP-codoped glasses are measured. The $\tau(^4I_{13/2})$ value significantly decreases when the glass is codoped with Pr^{3+}. The experimental values of $\tau_{Er/Pr}$ and τ_{Er} are 3.23 ms and 731 μs, respectively. When the concentration of Pr^{3+} is 0.2 mol%, the lifetime of $^4I_{13/2}$ is too low to determine. This result suggests that $\tau(^4I_{13/2})$

is significantly quenched by Pr^{3+} ions. The quenched $^4I_{13/2}$ lifetime indicates energy transfer to Pr^{3+}[12]. Lifetime quenching of $^4I_{13/2}$ also explains the energy transfer between Er^{3+} and Pr^{3+}. The energy transfer efficiency, which is calculated as 77.4% in this letter, is defined in Ref. [13].

To investigate the energy transfer mechanism, the upconversion spectra of Er^{3+}- doped and EP-codoped glasses were obtained (Fig. 3). The green and red emission signals are evidently weaker in EP-codoped glass than in Er^{3+}-doped glass, which indicates that the ions of $^4I_{15/2}$ are excited to the $^4I_{11/2}$ state by ground-state absorption. Some ions in the $^4I_{11/2}$ and $^4I_{13/2}$ levels show an upconversion process (ETU). The energy stored in $^4F_{7/2}$ then decays nonradiatively into $^2H_{11/2}$, $^4S_{3/2}$, and $^4F_{9/2}$. As such, the green emission may be attributed to Er^{3+}: $^2H_{11/2} \rightarrow ^4I_{15/2}$, $^4S_{3/2} \rightarrow ^4I_{15/2}$, whereas the red emission is related to Er^{3+}:$^4F_{9/2} \rightarrow ^4I_{15/2}$. After addition of Pr^{3+} to the glass, the ETU process weakens because of the energy transfer processes Er^{3+}: $^4I_{11/2} \rightarrow$Pr^{3+}:$^1G_4$ (ET1) and Er^{3+}:$^4I_{13/2} \rightarrow$Pr^{3+}:$^3F_{3,4}$; hence, ions in the $^4I_{11/2}$ level are largely depopulated and 1.5-μm emission decreases. This process is shown in Fig. 4.

In this letter, oxygen gas bubbling and substitution of PbO by PbF$_2$ were applied to reduce OH$^-$ groups. According to Ref. [14], high contents of PbF$_2$ may damage
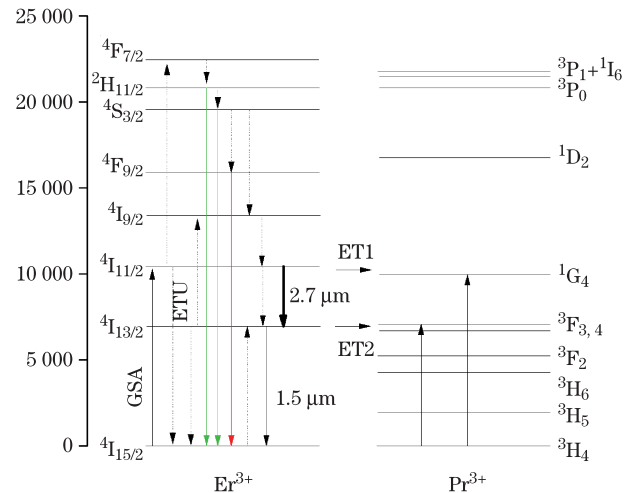

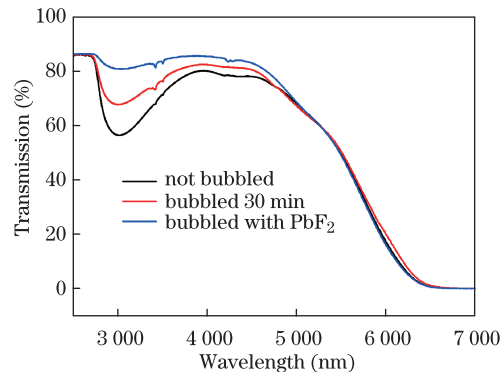Fig. 4. Mechanism of energy transfer in EP-codoped glass.

Fig. 5. Fourier-transform IR spectra of EP-codoped glass samples with and without 30-min bubbling and substitution of PbO by 3 mol% PbF$_2$.

Table 1. Spontaneous Transition Probability A of $^4I_{11/2}$ to $^4I_{13/2}$ and Emission Cross-sections at 2.7 μm in Various Glasses.

Glass Compositions	$A\,(^4I_{11/2} \to {}^4I_{13/2})(s^{-1})$	σ_e (cm^2)	References
Fluorophosphate	22.16	$(6.57\pm0.11)\times10^{-21}$	[17]
Fluoride	28.92	9.8×10^{-21}	[18]
Fluorotellurite	21.36	6.32×10^{-21}	[19]
Germanate	36.69	8.44×10^{-21}	This Letter

the thermal ability of glasses; thus, only 3 mol% PbF$_2$ was added to the glass. The OH$^-$ groups in the glass can be expressed in terms of the absorption coefficient α[15]. A description of the calculation of α can be found in Ref. [15]. The α of the bubbled sample with 3 mol% PbF$_2$ replacement is 0.67 cm^{-1}, which is lower than that of samples without PbF$_2$ (Fig. 5).

According to the emission spectra and Füchibauer–Ladenburg theory[16], the 2.7-μm emission cross-section is 8.44×10^{-21} cm^2, which is greater than that in fluorophosphate and fluorotellurite glasses. All of the results obtained in this work are listed in Table 1. The EP-codoped glass described in this letter consistently produces efficient 2.7-μm emission.

In conclusion, enhanced 2.7-μm emission is observed in EP-codoped germanate glass. The increase in concentration of Pr^{3+} ions is beneficial to the intensity of 2.7-μm PL. Thus, addition of Pr^{3+} is a practical approach for inducing efficient 2.7-μm emission in germanate glass. The decay time of Er^{3+}:$^4I_{13/2}$ and the upconversion spectra of EP-codoped glass suggest energy transfer between Er^{3+} and Pr^{3+}. The energy transfer mechanisms are discussed in detail, and the energy transfer efficiency is calculated as 77.4%. Judd–Ofelt theory and Füchibauer–Ladenburg calculation results show that the spontaneous transition probability of Er^{3+}:$^4I_{11/2} \to {}^4I_{13/2}$ is 36.69 s^{-1} and that the emission cross-section at 2.7 μm is 8.44×10^{-21} cm^2. These results suggest that EP-codoped germanate glass can be used to achieve efficient 2.7-μm emission.

References

1. M. Pollnan and S. D. Jackson, IEEE J. Selected Topics Quantum Electron. **7,** 30 (2001).
2. X. Zhu and R. Jain, Opt. Lett. **32,** 26 (2007).
3. S. Tokita, M. Murakami, S. Shimizu, M. Hashida, and S. Sakabe, Opt. Lett. **36,** 2812 (2011).
4. S. Tokita, M. Murakami, S. Shimizu, M. Hashida, and S. Sakabe, Opt. Lett. **34,** 3062 (2009).
5. L. Zhang, Z. Yang, Y. Tian, J. Zhang, and L. Hu, J. Appl. Phys. **110,** 093106 (2011).
6. H. Zhan, Z. Zhou, J. He, and A. Lin, Opt. Lett. **37,** 3408 (2012).
7. H. Lin, D. Chen, Y. Yu, A. Yang, and Y. Wang, Opt. Lett. **36,** 1815 (2011).
8. D. J. Coleman, S. D. Jackson, P. Golding, and T. A. King, J. Opt. Soc. Am. B **19,** 2927 (2002).
9. Y. Guo, M. Li, L. Hu, and J. Zhang, J. Phys. Chem. A **116,** 5571 (2012).
10. D. F. d. Sousa, J. A. Sampaio, L. A. O. Nunes, M. L. Baesso, A. C. Bento, and L. C. M. Miranda, Phys. Rev. B **62,** 3176 (2000).
11. X. Feng, S. Tanabe, and T. Hanada, J. Am. Ceram. Soc. **84,** 165 (2001).
12. P. S. Golding, S. D. Jackson, T. A. King, and M. Pollnau, Phys. Rev. B **62,** 856 (2000).
13. G. Bai, J. Ding, L. Tao, K. Li, L. Hu, and Y. H. Tsang, J. Non-Cryst. Solids **358,** 3403 (2012).
14. X. Jiang, J. Lousteau, S. Shen, and A. Jha, J. Non-Cryst. Solids **355,** 2015 (2009).
15. S. Guan, Y. Tian, Y. Guo, L. Hu, and J. Zhang, Chin. Opt. Lett. **10,** 071603 (2012).
16. S. A. Payne, L. L. Chase, L. K. Smith, W. L. Kway, and W. F. Krupke, IEEE J. Quantum Electron. **28,** 2619 (1992).
17. Y. Tian, R. Xu, L. Zhang, L. Hu, and J. Zhang, Opt. Lett. **36,** 109 (2011).
18. F. Huang, Y. Guo, Y. Ma, L. Zhang, and J. Zhang, Appl. Opt. **52,** 1399 (2013).
19. Y. Guo, G. Gao, M. Li, L. Hu, and J. Zhang, Mat. Lett. **80,** 56 (2012).